

A Single-Phase Tubular Flux-Switching Generator Analysis for Generating Electrical Energy from Walkways

Serdal Arslan¹

Abstract

Today, alternative methods are being sought for obtaining electrical energy via harvesters. One of these methods is the use of small powerful energy harvesters on walking paths, which has been an important research topic in recent years. For example, these harvesters can be used to obtain electrical energy from both daily walking and sports activities. Piezoelectric material systems generally used to obtain electrical energy from walking paths. Although their power values are in nano or micro values, it can be predicted that significant electrical energy will be gained during use. Electrical energy can also be obtained from systems integrated with linear generators positioned on the walking path. For these applications, both the single-phase model of the linear flux switched generator internal and external moving models have been compared.

1. INTRODUCTION

In our daily lives, the energy we expend because of our physical movements is going to waste. This has led to the search for systems that can generate electrical energy on a mini and micro scale for the recovery of expended energy. In other words, systems referred to as energy harvesting systems can meet our instantaneous energy needs. It is not expected that energy harvesting technologies alone will meet countries' increasing energy demands. However, they can meet the requirements of existing energy-consuming sensor systems. Considering that harvesting technology is relatively new, innovative applications for various fields are on the rise [1,2]. Energy harvesting from a biomechanical perspective in humans has been

1 Doç.Dr., Harran Üniversitesi Organize Sanayi Bölgesi M.Y.O. Elektrik Programı, serdalarlan@harran.edu.tr, 0000-0002-1187-5633

classified as piezoelectric, triboelectric, electromagnetic, and electrostatic [3]. Particularly, piezoelectric and thermoelectric systems can be used for energy harvesting when implanted in the body [4]. The daily power generation from human movements (hand, arm, or foot) of approximately 20-70W is noteworthy [5]. Portable, wearable, and even implantable harvesters are limited in terms of power, and power generated from the foot is quite high [5]. Integration of energy harvesting systems into transportation (road, rail, air, sea) systems is particularly interesting. Some key studies for these applications related to small-scale energy harvesting technologies can be summarized [6]:

- The installation of solar panels on highways to generate electrical energy [7]. Currently, there are issues related to installation and durability [6,8]. However, by using durable materials, warning LEDs can be powered to ensure the attention of vehicles in areas with pedestrian crossings [7].
- It is possible to generate electricity from wind energy in areas with heavy vehicle traffic [9].
- In hot climates, electricity can be generated through Thermoelectric Generators (TEGs) [6,8].
- Despite not being satisfactory in terms of output power, it is possible to generate energy from noise in places with high sound sources.
- There are extensive studies on energy harvesting using piezoelectric technology, primarily through vibrations. The power that can be obtained from this system is in the micro or milli range [1-8,10].
- Applications for energy harvesting systems can be diversified through electromechanical systems. Models in this field have mostly focused on energy production from mechanical systems or piezoelectric systems. It is possible to generate sufficient power for sensors and charging systems from these systems [1-8,10].

The Dutch start-up Energy Floors can be cited as the pioneer in this field. In 2008, they implemented the first application of converting kinetic energy from dancers into electricity at Club Watt, a sustainable dance club in Rotterdam [11]. Later, in 2014, they focused on electricity generation from a pedestrian floor that converts solar energy, known as the Smart Energy Floor [11]. These applications have become widespread at festivals, fairs, educational institutions, public transportation, and globally. In fact, these systems offer a new application area known as “Smart or Sustainable Floors.” Additionally, they can be designed for on-grid use, but these systems are often

used as off-grid interactive LED lighting or power sources. The harvested electrical energy from the system is used to power the electronic card, which includes sensors, motion detectors, and a charging control system.

One of their applications, “The Gamer,” focuses on promoting physical exercise in game parks through a solar-powered floor while simultaneously generating electrical energy [11]. Another company, Pavegen, founded in 2009, has a focus on interactive data collection as a “Smart or Sustainable Floor” [11]. They use this data to establish meaningful connections with individuals and companies. For instance, it’s possible to convert the data from smart footsteps into digital currency or brand-based discounts. Figure 1 provides simulations of a solar panel-based and an electromechanical energy-harvesting pedestrian pathway.

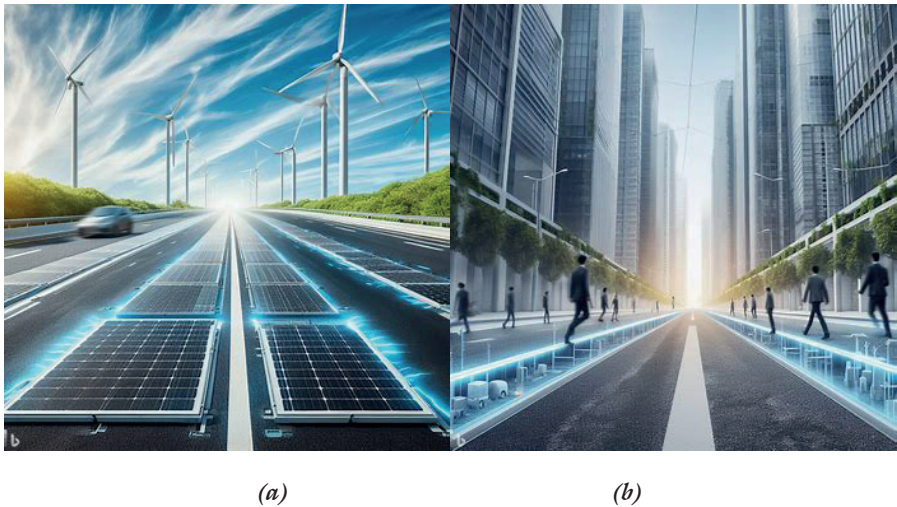


Figure 1. (a) Photovoltaic-based pedestrian pathway floor application², (b) Electromechanical-based pedestrian pathway floor application³ [12]

Most of these studies are aimed at meeting the energy needs of sensor systems. In this study, unlike other harvesting concepts (such as photovoltaic, wind, piezoelectric, electromagnetic, etc.), designs of linear generators driven by a moving mechanism have been considered. These systems typically generate electricity through walking, running, climbing, hand-arm

2 ²The images shown here are artificial intelligence-generated visuals related to energy harvesting from pedestrian pathways.

3 ³The images shown here are artificial intelligence-generated visuals related to energy harvesting from pedestrian pathways.

coordination, or forward-backward hand movements. Handheld harvesters (such as battery-less flashlights, etc.) or energy harvesting from natural walking or daily physical activities of humans are commonly preferred. For example, a mechanical system placed in a backpack for carrying loads generated 7.4W of power [13]. A controlled sliding system was proposed as a new harvester design [14]. Acceleration data at 3km/s for the sole of the foot, toe, and heel were examined. Additionally, five different linear generator designs were studied to obtain micro power for shoes [15]. For the shoe application, the pole ratio, shape ratio, inner and outer diameter ratios of the linear generator were parametrically examined, and suitable models were tested [16-17]. Sajwani et. al. [18] proposed a Halbach-arrayed linear generator as the harvester. Studies discussed in the literature have focused on portable, implantable, and wearable harvesting systems. However, the system considered in this article is based on energy generation through a generator that can be integrated into a pedestrian pathway. Electric power can be generated through a linear generator driven by a mechanical system depending on motion.

Linear generators can come in various types, including induction, permanent magnet, switched reluctance, and more [19]. Especially, permanent magnet generators are known for their high efficiency and power density, leading to increased research on machines based on permanent magnets and their variations. Based on magnet arrangement, they can be classified as Halbach arrayed, axial flux, and radial flux [20]. The Halbach arrangement increases the magnetic flux in the air gap and allows for smoother sinusoidal voltage output. Halbach arrangement consists of axial and radial flux magnets. Continuous magnet linear generators can be evaluated based on their moving parts, construction, and magnetic flux direction dependency [21]. The moving part can be composed of steel material, magnets, windings, or various combinations thereof. Depending on the condition of the stator and the moving part, it can be categorized as short or long stroke. It can also be classified as transverse or longitudinal according to the magnetic flux direction. Single-sided/double-sided construction has been studied for suspension systems [22], but more research has been conducted on the tubular structure due to its advantages (zero net radial forces, absence of end winding effects, etc.). The core structure of the stator or moving part can be made of iron or air. Iron core provides more power compared to air-core [23,24]. Flux-switching machines feature windings, magnets, and steel materials in the stator structure, while the moving part consists solely of steel material. This allows for mechanical robustness and cooling in the moving part [25]. A comparison has been made between the Halbach

arrayed tubular linear generator with a 9/10 slot/pole combination and the flux-switching tubular linear generator (FSTLG) [26], and the FSTLG with 12 slots/10 poles and 12 slots/14 poles structures has been examined [27]. The stator and moving steel materials of the FSTLG can be made of the same or different materials [28]. In another study, 6 slots/5 poles and 6 slots/7 poles FSTLGs have been investigated [29].

The selected linear generator topology should have a short stroke, occupy minimal space, be lightweight, provide good mechanical damping [30], and offer high output performance depending on speed changes [30], especially tailored to the intended use, the speed-frequency profile, and force values of the system may vary.

2. FSTLG STRUCTURE AND MODEL

This study considers the dimensional specifications of a multi-pole, three-phase tubular flux-switching generator that has been previously designed and implemented [31] (Table 1). Figure 3 shows a single-phase tubular flux-switching generator. Using one phase of the three-phase generator as a reference, inner runner and outer runner models have been created (Figure 2).

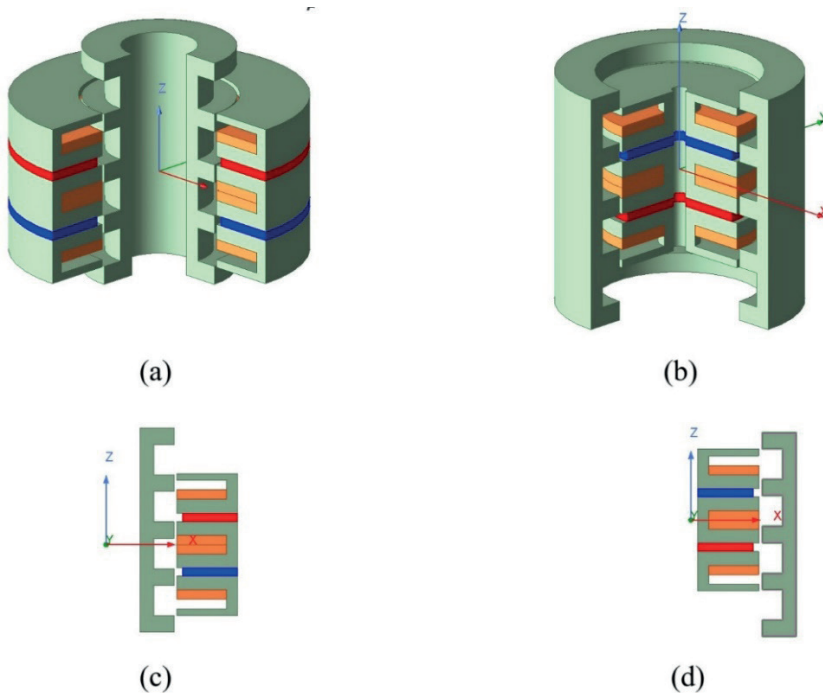


Figure 2. Flux-switching tubular linear generator models; a) 3D model of inner runner; b) 3D of outer runner; c) 2D-rz of inner runner; d) 2D-rz of outer runner

Figure 3 represents geometrical sizing of inner runner flux-switching tubular linear generator in rz coordinate system. Taking the inner radius into account, the outer runner model in Figure 2 was created. The primary and secondary dimensions of both models were taken equal.

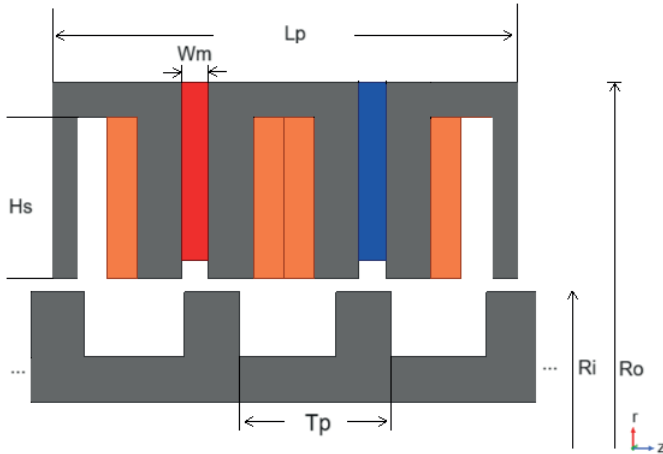


Figure 3. 2D representation of geometrical sizing of flux-switching tubular linear generator in rz coordinate system

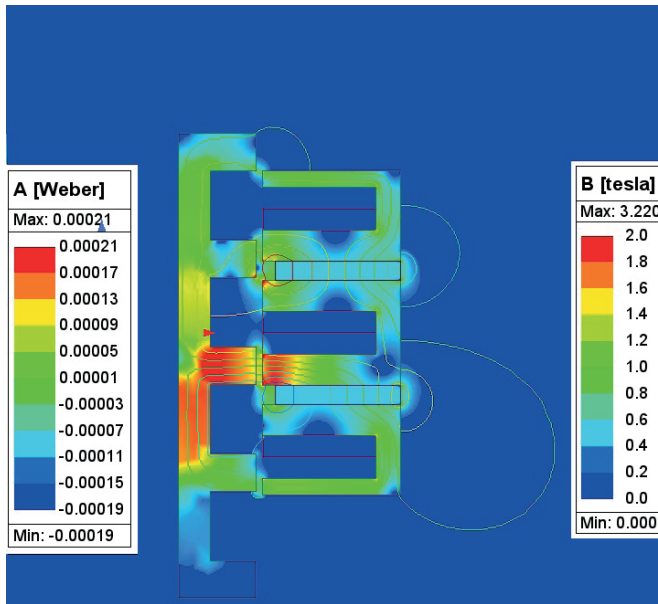
Information about the dimensional parameters shown in Figure 3 is provided in Table 1.

Table 1. Characteristics of the tubular linear generator geometric

Geometric	Values (mm)	Geometric	Definitions and Values (mm)
Primer length (L_p)	51.4	Primary and Secondary Steel Material	M43_29G
Pole pitch (T_p)	17	Permanent Magnet (PM) Type	NdFe35
Height slot (H_s)	18	Inner diameter to outer diameter ratio for tubular type	0.53
Magnet width (W_m)	3	Inner radius (R_i)	25.5mm
Winding Type	Double Layer	Air-gap length (g)	1mm

3. FINITE ELEMENT ANALYSIS RESULTS AND EVALUATION

For numerical analyses, the commercial software ANSYS Maxwell was used due to its wide-ranging capabilities, solver infrastructure, and established validity in the literature. Solving electromagnetic problems using the finite element method offers both high accuracy and time efficiency. The models presented in Figure 2c and Figure 2d were analysed using this software through numerical simulations. The analyses were performed on a computer with the following specifications: 12th Gen Intel(R) Core (TM) i7-12700H 2.30 GHz processor and 16GB of RAM. The mesh numbers for inner runner, outer runner models are listed as 59,400 and 630,592, respectively. The magnetic flux density distribution for magnetostatic analysis is shown in Figure 4.



(a)

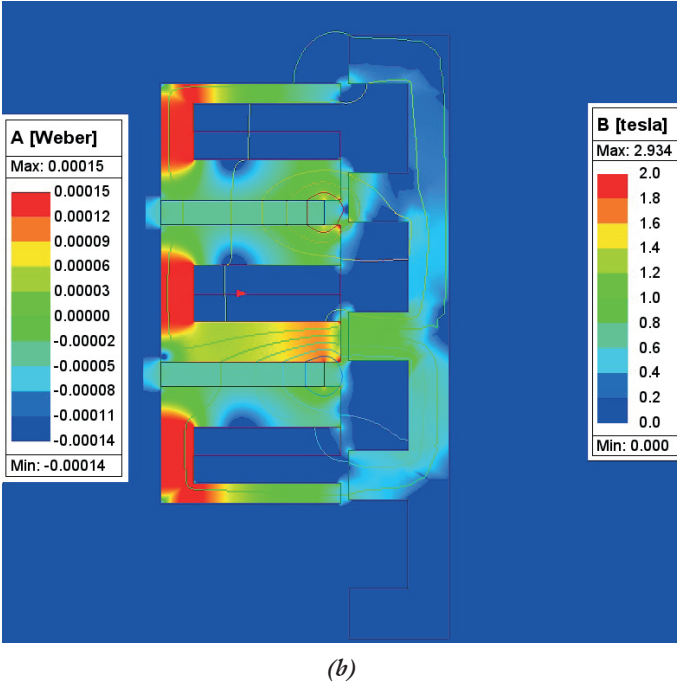


Figure 4. Magnetic flux density distribution, (a) Inner runner, (b) Outer runner

Here, similar changes in magnetic flux density were observed between the secondary teeth and magnet for both inner runner and outer runner models. However, in the inner runner model, an increase in magnetic flux density was observed in the moving steel compared to the outer runner model. Additionally, there is leakage flux at the upper and lower points of the magnet in all models, and these regions should be considered. Partial demagnetization can be occurred. In Figure 5, the flux density distribution in the air gap is similar for both models. However, it is observed that the inner runner model has a higher flux density. The flux density at 37.5 mm is 43% higher than the outer runner model.

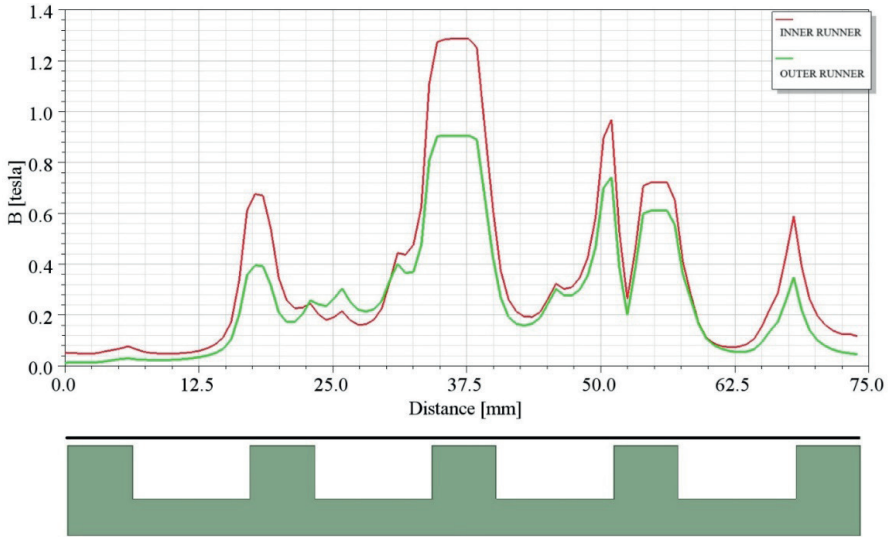


Figure 5. Magnetic field change along the in the middle of the gap

Transient analysis was performed for both models. In previous studies [32], the induced voltage increased as the speed increased. In this respect, no comparison was performed for variable velocities. In this context, the moving speed was taken as 1m/s. The inner radius was increased parametrically while keeping the velocity constant. The voltage induced in a phase winding was compared with the no-load operation (Figure 6).

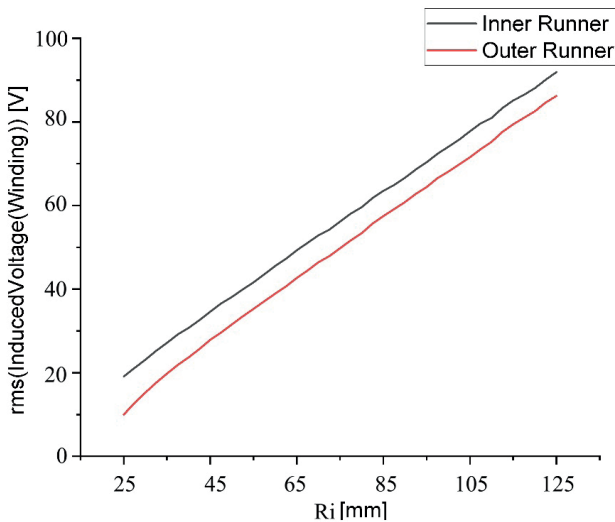


Figure 6. Induced voltage in the winding with R_i .

As the radius increases, the voltage induced in the winding increases linearly. While the V/mm ratio increases at the same rate, there is a difference in the induced voltage of approximately 7.4V.

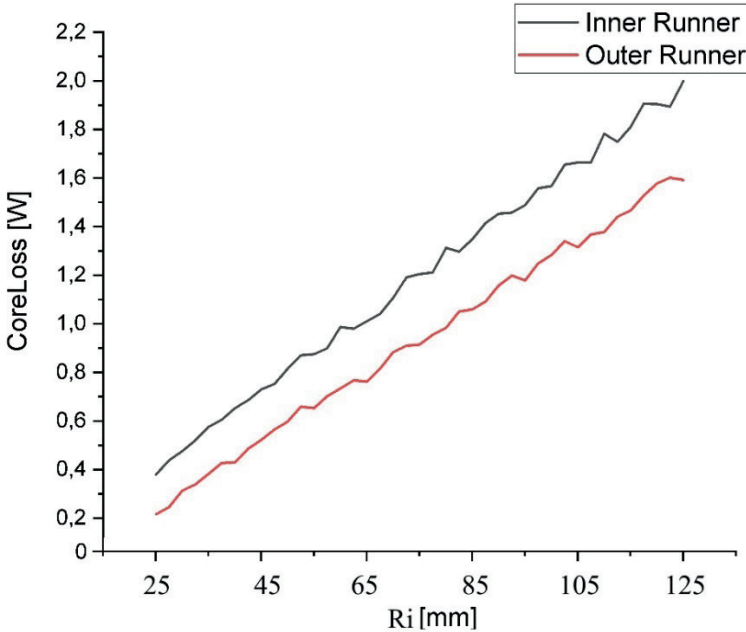


Figure 7. The core losses versus Ri

As the radius increases, iron loss increases. The internal moving (inner runner) model has more iron loss than the external moving (outer runner) one. This is due to the flux density. Although the air gap diameter of both models is equal, the phase resistance is not equal at the same number of turns. The internal moving model was loaded with a resistive load of 28.27 ohms and the external moving model with a resistive load of 14.13 ohms. Figure 8 was obtained according to the average value of the output power.

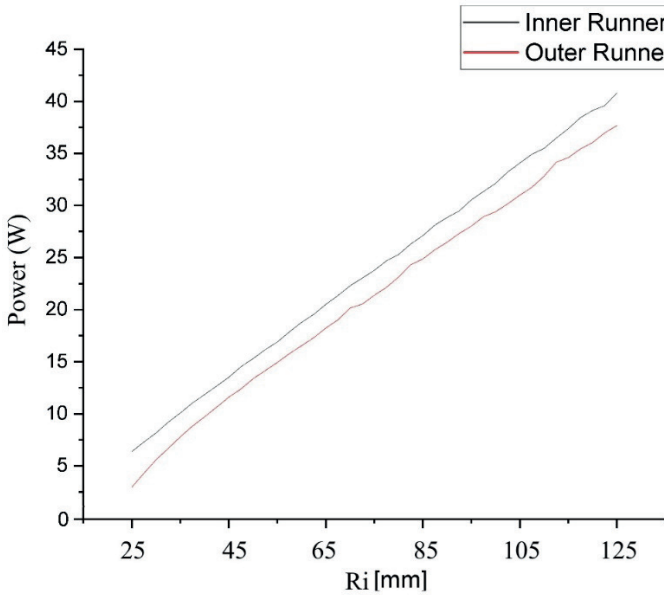


Figure 8. The power versus R_i

The unit cost values taken are 2.12 USD/kg for steel material, 14.85 USD/kg for copper material, and 84.87 USD/kg for magnet material (NdFeB) respectively [33]. The cost calculation presented in Table 2 does not include machine body and labor costs. Here, the primary steel density is taken as 7700 kg/m^3 , copper winding density as 8933 kg/m^3 , magnet density as 7400 kg/m^3 , and secondary steel density as 7700 kg/m^3 . Table 2 was prepared based on the data in Table 1.

Table 2. Material costs and mass of models

Models	Primary Iron Mass (kg)	Secondary Iron Mass (kg)	PM Mass (kg)	Cooper Mass (kg)	Total Mass (kg)	Total Cost (USD)
Inner Runner	1.150	0.483	0.209	0.474	2.316	28.23
Outer Runner	0.376	0.939	0.0697	0.212	1.596	11.851

When Table 2 is examined, the externally driven model is 31% less in terms of mass. Similarly, it is 58% less costly.

4. CONCLUSION

In this study, single-phase tubular flux-switching generator models for pedestrian walkways were analyzed. Simulation studies were conducted considering the single-phase condition of the three-phase generator subjected to tests. Analysing with the same dimensional parameters, the results showed that as the inner radius increased, the induced voltage in the winding also increased. In terms of core loss variation, inner runner showed higher variations compared to the outer runner model. However, the power exhibited only slight increments for inner runner. Although there is no significant difference in output power between the two models, it can be said that the externally driven model is the more suitable model in terms of cost and total weight.

Future work will involve multiphysics analyses of the designed models, followed by prototype manufacturing of the selected model. Experimental results will be obtained from the walking platform prepared for this purpose. This will enable the utilization of energy generated from activities such as walking, social activities, and playgrounds for local lighting and sensor systems.

Acknowledgment

The author would like to thank Ulupars Ltd. Şti. for financial support during the design and testing processes.

References

1. E. M. Nia, N. A. W. A. Zawawi, and B. S. M. Singh, "A review of walking energy harvesting using piezoelectric materials." IOP Conference Series: Materials Science and Engineering, IOP Publishing, 291, 1, 2017.
2. H. Akinaga, "Recent advances and future prospects in energy harvesting technologies," Japanese Journal of Applied Physics, 59,11, 2020.
3. I. Sobianin, S. D. Psoma, and A. Tourlidakis, "Recent Advances in Energy Harvesting from the Human Body for Biomedical Applications," Energies, 15,21, 2022.
4. T. M. Nidal, et al, "Recent Techniques for Harvesting Energy from the Human Body," Comput. Syst. Sci. Eng., vol. 40, 1, pp.167-177, 2022
5. H. Shi, Z. Liu, and X. Mei, "Overview of human walking induced energy harvesting technologies and its possibility for walking robotics," Energies, vol. 13, 1, 2019.
6. (2023) The Onio website. [Online]. Available: <https://www.onio.com/article/energy-harvesting-higway-roads.html>
7. Md. F. T. Hossain, et al, "Harvesting solar energy from asphalt pavement," Sustainability, vol. 13, 22, 2021.
8. E. H. H. Al-Qadami, Z. Mustaffa, and M.E. Al-Atroush, "Evaluation of the pavement geothermal energy harvesting technologies towards sustainability and renewable energy," Energies, vol. 15, 3, 2022.
9. (2023) The Elektrik Elektronik Egitimi website. [Online]. Available: <https://elektrikelektronikegitimi.blogspot.com/2018/06/istanbul-da-metrobus-ruzgarndan-elektrik.html>
10. R. Riemer, and A. Shapiro, "Biomechanical energy harvesting from human motion: theory, state of the art, design guidelines, and future directions," Journal of neuroengineering and rehabilitation, vol. 8, pp.1-13, 2011.
11. (2023) The Whatdesigncando website. [Online]. Available: <https://www.whatdesigncando.com/stories/why-not-use-our-pavements-and-roads-to-generate-energy/>
12. (2023) The Openai website. [Online]. Available: <https://openai.com/dall-e-3>
13. R. C. Lawrence, et al, "Generating electricity while walking with loads," Science, vol.309, pp.1725-1728, 2005.
14. H. Xia, et al, "Controlled slip" energy harvesting while walking," IEEE Transactions on Neural Systems and Rehabilitation Engineering, vol. 28, 2, pp.437-443, 2019.
15. P. Gui, et al, "Micro linear generator for harvesting mechanical energy from the human gait," Energy, vol.154 pp. 365-373, 2018.

16. J.-X. Shen, et al, "A shoe-equipped linear generator for energy harvesting," *IEEE Transactions on Industry Applications*, vol.49, 2, pp. 990-996, 2013.
17. CF Wang, et al, "A shoe-equipped linear generator for energy harvesting," *IEEE International Conference on Sustainable Energy Technologies (ICSET)*, 2010, p.1-6.
18. S.H., et al, "Hallbach array-based linear generator for human motion energy harvesting," *International Conference on Electrical and Computing Technologies and Applications (ICECTA)*, 2017, p.1-6.
19. S. Arslan, and O. Gurdal, "Polygonal tubular linear permanent magnet generator analysis and experimental test," *Scientia Iranica*, vol.29, 1, pp. 168-182, 2022.
20. A.S. Jalal, N. J. Baker, and D. Wu, "Design of tubular moving magnet linear alternator for use with an external combustion-free piston engine, vol. 6-6, 2016.
21. S. Arslan, "Overview of Generating Electricity from Wave Energy Systems and Investigation of Generator Topologies Used in Archimedes Wave Swing Systems," *International Conference on Natural Science and Engineering (ICNASE'16)*, 2016.
22. O. Shunsuke, "Basic characteristics of the linear synchronous generator using mechanical vibration of the automobile," *International Conference on Electrical Machines and Systems*, 2010, p. 1550-1554.
23. H. Li, and P. Pillay, "A methodology to design linear generators for energy conversion of ambient vibration," *IEEE Transactions on Industry Applications*, vol.47, pp.2445-2452, 2011.
24. B. LJ Gysen, et al, "Design aspects of an active electromagnetic suspension system for automotive applications," *IEEE transactions on industry applications* vol. 45, pp.1589-1597, 2009.
25. M. Kang, et al., "A new tubular fault-tolerant permanent-magnet motor for active vehicle suspension," *IECON 2012-38th Annual Conference on IEEE Industrial Electronics Society*, 2012, p. 4082-4086.
26. J. Wang, et al., "Comparative studies of linear permanent magnet motor topologies for active vehicle suspension," *IEEE Vehicle Power and Propulsion Conference*, 2008, p. 1-6.
27. J. Wang, et al., "Design considerations for tubular flux-switching permanent magnet machines," *IEEE Transactions on Magnetics*, vol. 44, pp.4026-4032, 2008.
28. Y. Putgul, and D. Altiparmak, "Vehicle Suspension System Types and Their Effects on Front Axle Geometry," *Journal of Polytechnic-Politeknik Dergisi*, vol.19, 2, 2016.

29. I. Martins, et al., "Permanent-magnets linear actuators applicability in automobile active suspensions," *IEEE Transactions on vehicular technology*, vol.55, pp.86-94, 2006.
30. B. Ebrahimi, "Development of hybrid electromagnetic dampers for vehicle suspension systems," Doctoral Thesis, Mechanical and Mechatronics Engineering, University of Waterloo, Canada, 2009.
31. S. Arslan, "Optimizasyon vasıtasıyla tüp tipi akı anahtarlamalı doğrusal jeneratörün vuruntu kuvveti azaltımı," *Academic Perspective Procedia*, vol.2, pp.668-676, 2019.
32. S. Arslan, "Developing a Tubular Type Flux-Switching Permanent Magnet Linear Machine for a Semi-active Suspension Systems." *International Journal of Automotive Technology*, 1-14, 2024.
33. G. Du, et al., "Comprehensive Comparative Study on Permanent-Magnet-Assisted Synchronous Reluctance Motors and Other Types of Motor," *Applied Sciences*, vol.13, 14, 2023.

